Assessment of Local Blowing and Suction in a Turbulent Boundary Layer

Kyoungyoun Kim,* Hyung Jin Sung,†
and Myung Kyoon Chung‡
Korea Advanced Institute of Science and Technology, Taejon 305-701, Republic of Korea

Introduction

WALL blowing or suction through a spanwise slot in a turbulent boundary layer has been frequently employed because of its possibility for turbulence control. A literature survey reveals that many experimental studies have been made on turbulent boundary layers subjected to a concentrated wall suction[1] and blowing.[2] Direct numerical simulations were performed for testing the local wall blowing/suction in turbulent channel[3] and boundary layer.[4] It was found that when wall blowing is applied through a spanwise slot turbulent motions are enhanced with increasing turbulent shear stress, while suction diminishes turbulent fluctuations.

To assess the effect of blowing/suction on the downstream development of the flow, a measure of the local blowing/suction rate is generally used:

$$\sigma \equiv \frac{v_w b}{U_\infty \theta_{\text{slot}}} \tag{1}$$

where v_w is the blowing/suction velocity, b is the streamwise width of the spanwise slot, and θ_{slot} is the momentum thickness of the unperturbed flow at the slot location.[1,4] This quantity σ represents the ratio of momentum flux gain/loss caused by the blowing/suction to momentum flux of the incoming boundary layer.[1] A perusal of the relevant literature indicates that σ has been employed as a principal parameter to define the local blowing/suction.[1,5] For example, Antonia et al.[1] reported that the minimum value of skin friction decreases linearly with increasing $|\sigma|$ when the suction rate is sufficiently high ($\sigma \leq -2.6$). Sano and Hirayama[5] demonstrated that the slot width hardly affects the turbulence characteristics as well as the velocity profiles when σ is fixed at a constant value.

Although σ has been employed as a representative parameter, it is necessary to further investigate the effect of v_w on the perturbed flow. From the definition of $\sigma \equiv v_w b/U_\infty \theta_{\text{slot}}$, the role of v_w is significant even though σ is constant. This can be easily detected from the momentum integral equation

$$\frac{\mathrm{d}\theta}{\mathrm{d}x} = \frac{c_f}{2} + \frac{v_w}{U_\infty} + \frac{1}{\rho U_\infty^2}\int_0^\infty \frac{\partial P}{\partial x}\,\mathrm{d}y \tag{2}$$

where v_w is closely related with the pressure gradient $\partial P/\partial x$, the skin friction c_f, and the momentum thickness θ of the perturbed flow. The purpose of the present study is to evaluate the role of v_w at a fixed value of σ. Emphasis is placed on the relaxation of the perturbed flow. An understanding of the relaxation is of prime importance in analyzing the effect of blowing/suction through a spanwise slot, where the blowing/suction is applied only over a limited spatial extent. Three different blowing/suction velocities are applied at the slot. Toward this end, a direct numerical simulation of turbulent boundary layer is performed. The recovery process of the perturbed flow is examined in terms of the mean flow characteristics and the wall pressure fluctuations.

Received 30 April 2001; revision received 24 September 2001; accepted for publication 24 September 2001.

*Ph.D. Student, Department of Mechanical Engineering, 373-1, Kusong-dong, Yusong-ku.

†Professor, Department of Mechanical Engineering, 373-1, Kusong-dong, Yusong-ku; hjsung@kaist.ac.kr. Member AIAA.

‡Professor, Department of Mechanical Engineering, 373-1, Kusong-dong, Yusong-ku.

Computational Details

As mentioned earlier, a direct numerical simulation of turbulent boundary layer is performed to test the flow. A schematic diagram of the computational domain is displayed in Fig. 1. The domain size is $200\theta_{\text{in}} \times 30\theta_{\text{in}} \times 40\theta_{\text{in}}$ in the streamwise, wall-normal, and spanwise directions, where θ_{in} is the momentum thickness at the inlet. Realistic velocity fluctuations at the inlet are provided by using the method of Lund et al.,[6] and the convective outflow condition is used for the outflow boundary condition. A no-slip boundary condition is imposed at the solid wall. At the freestream $u = U_\infty$, and $\partial v/\partial y = \partial w/\partial y = 0$ are applied. The periodic boundary conditions are used in the spanwise direction. The governing Navier–Stokes and continuity equations are integrated in time by using a fractional step method with an implicit velocity decoupling procedure.[7] A second-order central difference scheme is used in space with a staggered mesh. The Reynolds number based on θ_{in} and U_∞ is $Re = 300$, and the mesh contains $257 \times 65 \times 129$ points. The mesh is uniform in the streamwise and spanwise directions, whereas a hyperbolic tangent stretching is used in the normal direction to cluster points near the wall. In wall units the mesh resolution is $\Delta x^+ \simeq 12.40$, $\Delta y^+_{\min} \simeq 0.17$, $\Delta y^+_{\max} \simeq 23.86$, and $\Delta z^+ \simeq 4.96$, based on the friction velocity at the inlet. The computational time step $\Delta t U_\infty/\theta_{\text{in}}$ is 0.3 ($\Delta t^+ \simeq 0.25$), and the statistical quantities are sampled at every fifth time step and averaged for $3000\theta_{\text{in}}/U_\infty$ ($\simeq 2517\nu/u_\tau^2$).

Results and Discussion

For a fixed $|\sigma| = 0.322$ three different blowing/suction velocities are imposed through the slot, $|v_w|/U_\infty = 0.01242$, 0.02425, and 0.04630. Because σ is fixed, the streamwise width of the slot is inversely proportional to v_w, i.e., $v_w b = \text{const}$. The center of the slot for all cases is located at $x/\theta_{\text{in}} = 83.2$. The detailed blowing/suction conditions are listed in Table 1. To examine the effect of local blowing/suction, streamwise variations of the mean wall pressure are displayed in Fig. 2. For blowing, the adverse pressure gradient appears before and after the slot, whereas the favorable pressure gradient occurs above the slot. For suction the opposite is observed. This feature is consistent with the result of Park and Choi.[4] A closer inspection of the wall pressure recovery after the slot discloses that the recoveries for blowing collapse well on the same recovery line. However, the recovery processes for suction are different, i.e., each wall pressure recovers just after the slot.

To characterize these different recovery processes, the behaviors of each term in Eq. (2) are plotted in Fig. 3. At the inlet ahead of the slot, a canonical relation of turbulent boundary layer is satisfied, i.e., $c_f/2 = \mathrm{d}\theta/\mathrm{d}x$. Near the slot, however, the variations

Table 1 Blowing/suction conditions

$\lvert v_w/U_\infty \rvert$	Slot width	b/θ_{in}
0.01242	$67.2\theta_{\text{in}} \sim 99.2\theta_{\text{in}}$	32.0
0.02425	$75.0\theta_{\text{in}} \sim 91.4\theta_{\text{in}}$	16.4
0.04630	$78.9\theta_{\text{in}} \sim 87.5\theta_{\text{in}}$	8.6

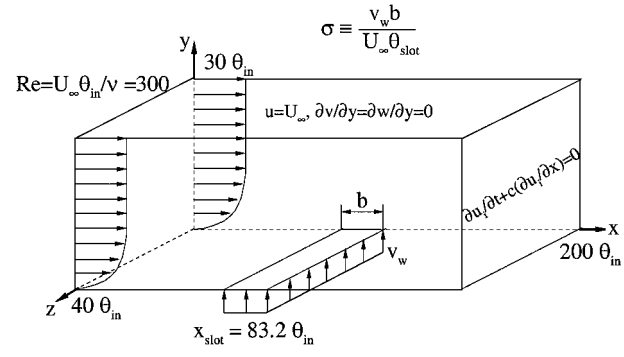

Fig. 1 Schematic diagram of the computational domain.

of $\int(\partial P/\partial x)\,\mathrm{d}y$ and $-\mathrm{d}\theta/\mathrm{d}x$ are significant because of the blowing/suction. For blowing a local maximum of $\int(\partial P/\partial x)\,\mathrm{d}y$ appears after the slot, and it increases with increasing v_w. It is remarkable to find that the maximum points are located at the same position ($x/\theta_{\mathrm{in}} \simeq 104$). However, the behaviors of $\int(\partial P/\partial x)\,\mathrm{d}y$ for suction in Fig. 3b show that the pressure gradients monotonously recover to zero just after the slot. The behaviors of $\int(\partial P/\partial x)\,\mathrm{d}y$ are similar to those of the mean wall pressure in Fig. 2. The streamwise variation of $c_f/2$ for blowing is much smaller than for suction.

It is important to examine the downstream turbulence quantities that arise as a result of the blowing/suction. The streamwise variations of $\Delta p'_{w,\mathrm{rms}} (=\sqrt{p'^2_w} - \sqrt{p'^2_{w,0}})$ for blowing/suction are exhibited in Fig. 4. Here, the subscript 0 stands for no blowing/suction. As shown in Fig. 4, the effect of the blowing/suction is significant. For blowing $\Delta p'_{w,\mathrm{rms}}$ increases after the slot, whereas it decreases for suction. As similar to that shown in Fig. 3a, the distributions of $\Delta p'_{w,\mathrm{rms}}$ have a local maximum after the slot for blowing. It is also found that the maximum points are located at the same position ($x/\theta_{\mathrm{in}} \simeq 104$) for three blowing cases.

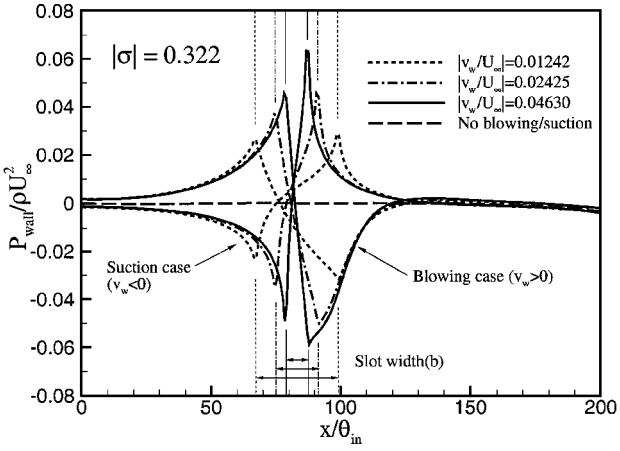

Fig. 2 Variations of mean wall pressure at $|\sigma|$ (=0.322).

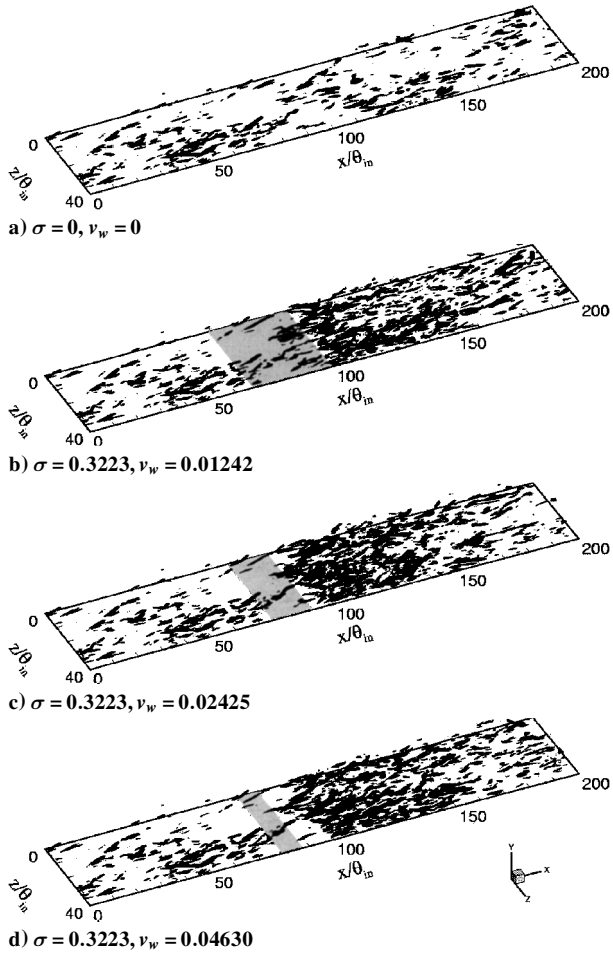

a) $\sigma = 0$, $v_w = 0$

b) $\sigma = 0.3223$, $v_w = 0.01242$

c) $\sigma = 0.3223$, $v_w = 0.02425$

d) $\sigma = 0.3223$, $v_w = 0.04630$

Fig. 5 Three-dimensional views of the streamwise vortices very near the wall for blowing (isosurfaces of $|\omega_x| = 0.35U_\infty/\theta_{\mathrm{in}}$): a) no blowing, b) $v_w/U_\infty = 0.01242$, c) $v_w/U_\infty = 0.02425$, and d) $v_w/U_\infty = 0.04630$.

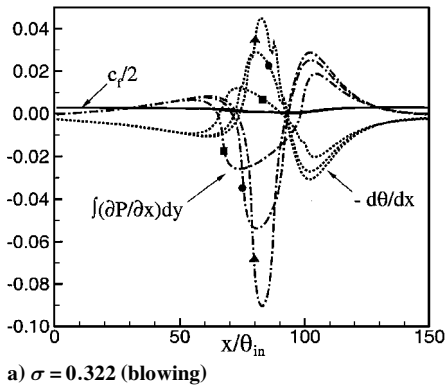

a) $\sigma = 0.322$ (blowing)

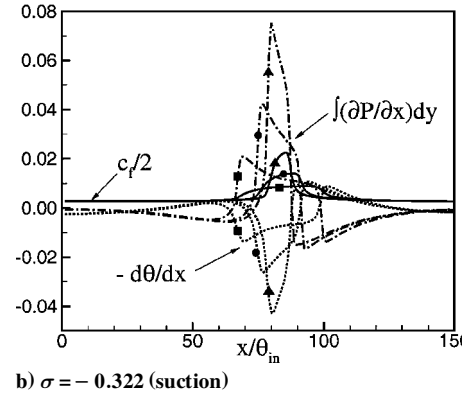

b) $\sigma = -0.322$ (suction)

Fig. 3 Variations of terms in the momentum integral equation: ■, $|v_w| = 0.01242U_\infty$; ●, $|v_w| = 0.02425U_\infty$; and ▲, $|v_w| = 0.04630U_\infty$.

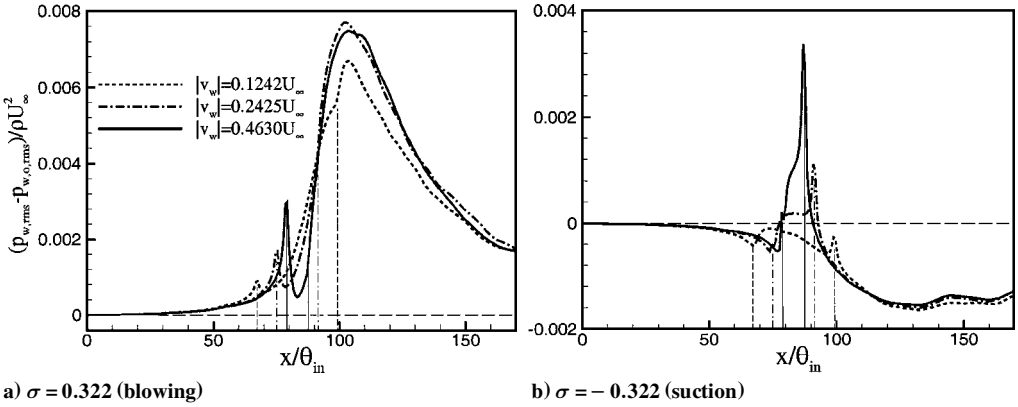

a) $\sigma = 0.322$ (blowing)

b) $\sigma = -0.322$ (suction)

Fig. 4 Variations of the rms of wall pressure fluctuations. Vertical lines denote the spanwise slot.

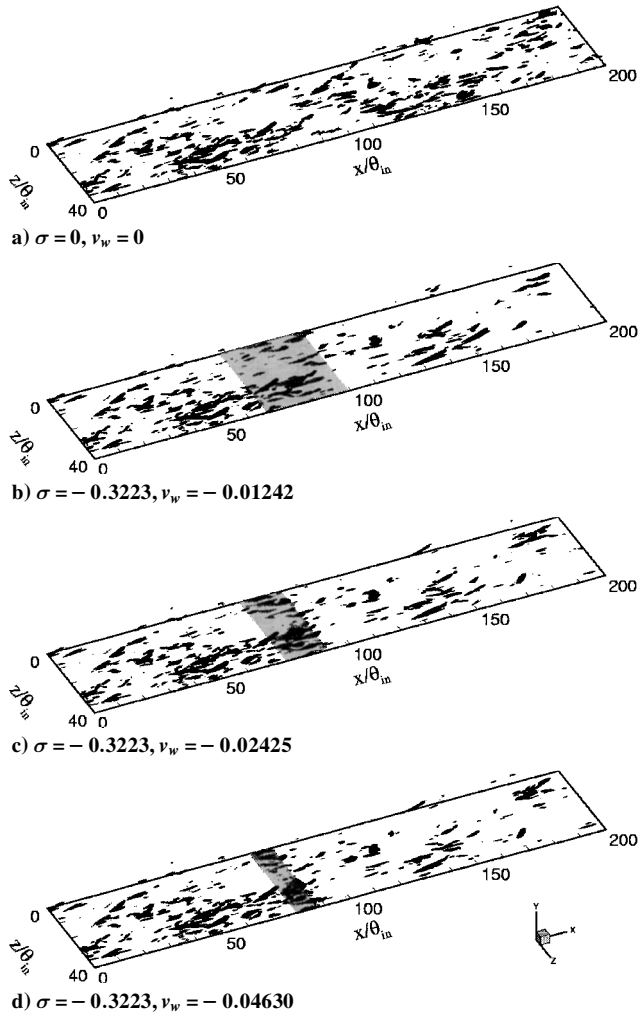

a) $\sigma = 0$, $v_w = 0$

b) $\sigma = -0.3223$, $v_w = -0.01242$

c) $\sigma = -0.3223$, $v_w = -0.02425$

d) $\sigma = -0.3223$, $v_w = -0.04630$

Fig. 6 Three-dimensional views of the streamwise vortices very near the wall for suction (isosurfaces of $|\omega_x| = 0.35U_\infty/\theta_{in}$): a) no suction, b) $v_w/U_\infty = -0.01242$, c) $v_w/U_\infty = -0.02425$, and d) $v_w/U_\infty = -0.04630$.

Three-dimensional views of the streamwise vortices very near the wall are illustrated in Figs. 5 and 6. These instantaneous flow visualizations are helpful in capturing the global effect of v_w on the flow. The contour values of ω_x are $|\omega_x| = 0.35U_\infty/\theta_{in}$. The regions of blowing/suction are denoted in gray. For blowing (Fig. 5) the vortical structures are lifted up above the slot and become much stronger downstream.[4] An interesting finding is that the strengthened near-wall vortices are accumulated at $x/\theta_{in} \simeq 107$, regardless of v_w. The maximum $\Delta\omega'_{x,rms} (= \sqrt{\omega'^2_x} - \sqrt{\omega'^2_{x,0}})$ is located at $(x/\theta_{in}, y^+_{in}) \simeq (107, 15)$ for three blowing cases. For suction (Fig. 6), however, the vortical structures are drawn toward the wall above the slot and become weaker downstream.[4] Because of the suction, the near-wall vortices are substantially weakened at the immediate rear of the slot. Just after the suction, they begin to recover without relaxation. This reflects that $\int (\partial P/\partial x)\, dy$ and $\Delta p'_{w,rms}$ recover monotonously for suction as shown in Figs. 3b and 4b.

Conclusions

The role of v_w at a fixed value of σ is tested for blowing/suction. Toward this end, a direct numerical simulation of turbulent boundary layer is performed at $Re_\theta = 300$. The results for three different values of v_w at a constant $|\sigma| = 0.322$ reveal that $|\Delta p'_{w,rms}|$ and $|\int (\partial P/\partial x)\, dy|$ increase with increasing $|v_w|$ above the slot. A local maximum exists after the slot for blowing. The local maxima for three blowing cases are located at the same position $(x/\theta_{in} \simeq 104)$. The streamwise variation of $c_f/2$ for blowing is much smaller than for suction. For blowing the strengthened near-wall vortices are accumulated at $x/\theta_{in} \simeq 107$, regardless of v_w. For suction, however, the near-wall vortices are weakened at the immediate rear of the slot.

Acknowledgment

This research was supported by a grant from the National Research Laboratory of the Ministry of Science and Technology, Republic of Korea.

References

[1] Antonia, R. A., Zhu, Y., and Sokolov, M., "Effect of Concentrated Wall Suction on a Turbulent Boundary Layer," *Physics of Fluids*, Vol. 7, No. 10, 1995, pp. 2465–2474.

[2] Krogstad, P. Å., and Kourakine, A., "Some Effects of Localized Injection on the Turbulence Structure in a Boundary Layer," *Physics of Fluids*, Vol. 12, No. 11, 2000, pp. 2990–2999.

[3] Chung, Y. M., and Sung, H. J., "Initial Relaxation of Spatially Evolving Turbulent Channel Flow with Blowing and Suction," *AIAA Journal*, Vol. 39, No. 11, 2001, pp. 2091–2099.

[4] Park, J., and Choi, H., "Effects of Uniform Blowing or Suction from a Spanwise Slot on a Turbulent Boundary Layer Flow," *Physics of Fluids*, Vol. 11, No. 10, 1999, pp. 3095–3105.

[5] Sano, M., and Hirayama, N., "Turbulent Boundary Layers with Injection and Suction Through a Slit. First Report: Mean and Turbulence Characteristics," *Bulletin of the Japan Society of Mechanical Engineering*, Vol. 28, No. 239, 1985, pp. 807–814.

[6] Lund, T. S., Wu, X., and Squires, K. D., "Generation of Turbulent Inflow Data for Spatially-Developing Boundary Layer Simulation," *Journal of Computational Physics*, Vol. 140, 1998, pp. 233–258.

[7] Kim, K., Baek, S.-J., and Sung, H. J., "An Implicit Velocity Decoupling Procedure for the Incompressible Navier–Stokes Equations," *International Journal for Numerical Method in Fluids* (to be published).

P. R. Bandyopadhyay
Associate Editor

Surface-Shear-Stress Pulses in Adverse-Pressure-Gradient Turbulent Boundary Layers

V. A. Sandborn*
Colorado State University,
Fort Collins, Colorado 80523-1320

I. Introduction

LARGE-MAGNITUDE surface-shear-stress pulses, which are present in all turbulent boundary layers, do not appear to be accounted for in current turbulence models. The pulses are related to the "sweep" motions observed near the surface in shear flows. These pulses are not only large in amplitude, but also the highest frequencies present. Thus, low-frequency (large-eddy) simulation models might not be able to capture them.[1]

Surface hot-wire evaluations of the time-dependent surface shear stress were employed to identify characteristic magnitudes and times for the pulses.

II. Experimental Results

Figure 1 shows a typical time trace of the surface shear stress obtained in an adverse-pressure-gradient turbulent boundary layer. The trace was for flow along a curved floor in a 61 × 61-cm wind tunnel (see Ref. 2 for experimental setup). Figure 2 shows the pressure-gradient variations along the curved floor for a number of Reynolds numbers (q is the upstream dynamic pressure). "Intermittent" turbulent separation occurred near the end of the curved

Received 9 September 2000; revision received 14 July 2001; accepted for publication 14 September 2001.

*Emeritus Professor, Civil Engineering. Senior Member AIAA.